Interaction between Stimulated Raman Scattering and Ion-Acoustic Waves in Ignition-Relevant Plasmas

R. K. Kirkwood   B. B. Afeyan[**]   K. G. Estabrook   M. A. Blain[***]

B. J. MacGowan   W. L. Kruer   C. A. Back   E. A. Williams

D. S. Montgomery[*]   J. D. Moody   S. H. Glenzer   R. L. Berger

B. F. Lasinski

Introduction

The transport of intense laser beams through large regions of underdense plasmas is important to achieving ignition by indirect-drive inertial confinement fusion (ICF).[1] The energy deposition profile of the laser beam in the target is strongly affected by stimulated scattering from ion-acoustic and Langmuir waves in the plasma created when the target material ionizes. These interactions are most simply modeled by the three-wave decay processes of stimulated Brillouin scattering (SBS) and stimulated Raman scattering (SRS), respectively.[2] The three-wave decay models assume that waves propagating in the plasma do not interact, that is, that the plasma response to the ponderomotive force of the incident and scattered light is linear. However, previous experimental observations[3,4] and theoretical studies[5–13] provide evidence that the Langmuir waves and the ion-acoustic waves are not independent. In fact, in the high-temperature, high-Z plasmas present in indirect-drive targets,[1] secondary decay instabilities can limit the SRS.[9–13] In these secondary processes, the Langmuir wave produced by the SRS process can itself decay into an ion-acoustic wave and either a secondary Langmuir wave (LDI) or a secondary electromagnetic wave (EDI), thus coupling the properties of the Langmuir wave directly to the properties of the ion-acoustic wave. The mechanism for limiting SRS reflectivities by LDI was first described by Karttunen[9] and Heikkinen and Karttunen,[10] and was later invoked to explain the SRS spectrum from Au foil plasmas.[11] These processes were subsequently shown to occur in numerical simulations.[7,8,12] Recently, Baker[13] suggested that EDI may also result in a limit to the reflectivity.

This article describes the first demonstration that the SRS reflectivity in a plasma can depend directly on ion-wave damping, and finds that under conditions similar to what is expected in ignition experiments, the SRS reflectivity is consistent with Langmuir wave amplitudes that are limited by a secondary decay. The experiments are done in a low-density Xe gas target plasma, in which C_5H_{12} is added as a low-Z impurity.[14] Measurements of x-ray spectra and transmitted light and calculations show that variation of the concentration of impurities below 10% has very little effect on the electron density n_e, temperature T_e, or collisional absorption rate, while calculations indicate that the impurities have a large effect on the ion-wave damping. The SRS reflectivity, or equivalently the Langmuir wave amplitude, is found to depend on the impurity concentration and thus on ion-wave damping, and to track the threshold for decay of the Langmuir wave. The plasmas produced in these experiments mimic the properties of those that form near the wall in a Au hohlraum filled with a low-Z gas, such as will be used in ignition experiments on the National Ignition Facility (NIF) at somewhat lower laser intensity.[1] These open geometry targets also provide a uniform and well characterized plasma. Other experiments in gas-filled hohlraums have also shown a dependence of SRS on ion-wave damping, both when the wall is doped with a Be impurity to mimic the gradients and time dependence of the wall plasma expected in NIF experiments,[15] and when the gas has large fractions of both low- and high-Z material.[16] However, plasma properties vary along the ray path in those experiments, making identification of the physical mechanism difficult.

*   Los Alamos National Laboratory, Los Alamos, NM.
**   University of California at Davis, Davis, CA.
*** Centre D'Etudes de Limeil–Valenton, France.

Experimental Design

The experiments were conducted on the Nova laser in an approximately spherical plasma produced by nine $f/4.3$, = 351 nm beams. These heater beams each produce 2.5 TW of power continuously for 1 ns, with a total power of 22.5 TW. The beams pass through a gas mixture at 1 atm of pressure contained inside a 260-nm-thick spherical polyimide shell with radius r_0 = 1.3 mm.[17] The heater beams are aligned to cross at the center of the target. The heaters are defocused such that they are converging with a beam radius that is approximately equal to the target radius, providing spatially uniform heating. The electrons are heated to a temperature of T_e = 3.6 keV during the t = 0.5- to 1.0-ns period when the plasma parameters are most constant in space and time.[17] The electron density n_e is determined by the initial gas density and the average charge state. At this temperature, Xe has a charge state of about 40,[18] leading to n_e = 8.5×10^{20} cm^{-3}. Since the C_5H_{12} impurity is fully ionized and carries 42 electrons per molecule, n_e is independent of its concentration to within 5%. T_e is determined from measurements of x-ray line ratios and x-ray transport modeling as described in Ref. 18 and is in agreement with LASNEX[19] simulations. Measurements of radiated power and beam attenuation by collisional absorption indicate that T_e is also insensitive to impurity concentration. The measured transmission of a beam through the plasma[20] varies only from 1% to 2% when the impurity concentration is varied from 0% to 30%, and is also in agreement with the simulations, similarly indicating that the T_e variations are small ($\pm 6\%$). Measurements of the radiated x-ray power in the photon energy range of 0.2 to 2 keV[21] indicate that the radiated power is also constant within $\pm 15\%$ over the same range of impurity concentration. The lack of dependence of n_e and T_e on impurity concentration indicates that the frequency and damping rate of the Langmuir wave are also constant.

An interaction beam produces 1.5 TW continuously for 1.0 ns with = 351 nm. This beam is delayed 0.5 ns with respect to the heaters and is focused at the plasma center. Reflectivity measurements are made during the 0.5- to 1.0-ns (early) period when the heaters are on, as well as during the 1.0- to 1.5-ns (late) period when the plasma is cooling and less homogeneous. The interaction beam is smoothed by a random phase plate and by 0.7-Å FM bandwidth dispersed across the beam in the near-field that smoothes by spectral dispersion (SSD), so that its peak intensity and spot size in vacuum are 7.0×10^{15} W/cm^2 and 177 μm full width at half maximum (345 μm between first Airy minima). The plasma properties encountered by the interaction beam during the early period are calculated by LASNEX[19] for a 90% Xe, 10%

C_5H_{12} gas mix, indicating a T_e and n_e plateau near the plasma edge, as shown in Figure 1. The classical collisional absorption length for 351-nm light in Xe with a 3.6-keV T_e and 8.5×10^{20}-cm^{-3} n_e is 800 μm. Therefore, the majority of the backscattering occurs outside r = 0.5 mm. The downshifted light scattered within 20° of direct backscatter is measured[22] with a streaked optical spectrometer in the visible, with a spectral range of 400 to 700 nm, and a second spectrometer in the ultraviolet, with a spectral range of 346 to 361 nm. The SRS light detected by the long-wavelength spectrometer from an experiment with 5.5% C_5H_{12} impurity is shown in Figure 2. During the early period, the peak of the spectrum is at 575 nm, consistent with scattering from a Langmuir wave propagating in a plasma with an electron density n_e equal to 10% of the critical density n_c and a 3.0-keV T_e comparable to the simulated plasma parameters near r = 1.2 mm. After the heaters turn off at 1.0 ns, the peak shifts to the blue, indicating cooling and expansion of the plasma.
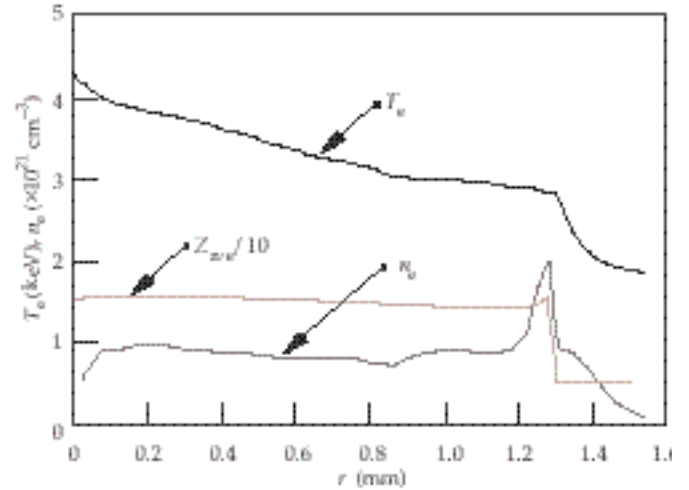

FIGURE 1. Calculated electron density n_e, electron temperature T_e, and averaged ionization state at t = 0.7 ns indicate that n_e and T_e scale lengths are long.   (08-00-0797-1243pb01)

Observations of Scattering vs Ion-Wave Damping

Experiments were performed with six different impurity concentrations between 0% and 30% C_5H_{12} and exhibit a strong dependence of the SRS reflectivity on the concentration of C_5H_{12}, which is interpreted as a dependence of Langmuir wave amplitude on the
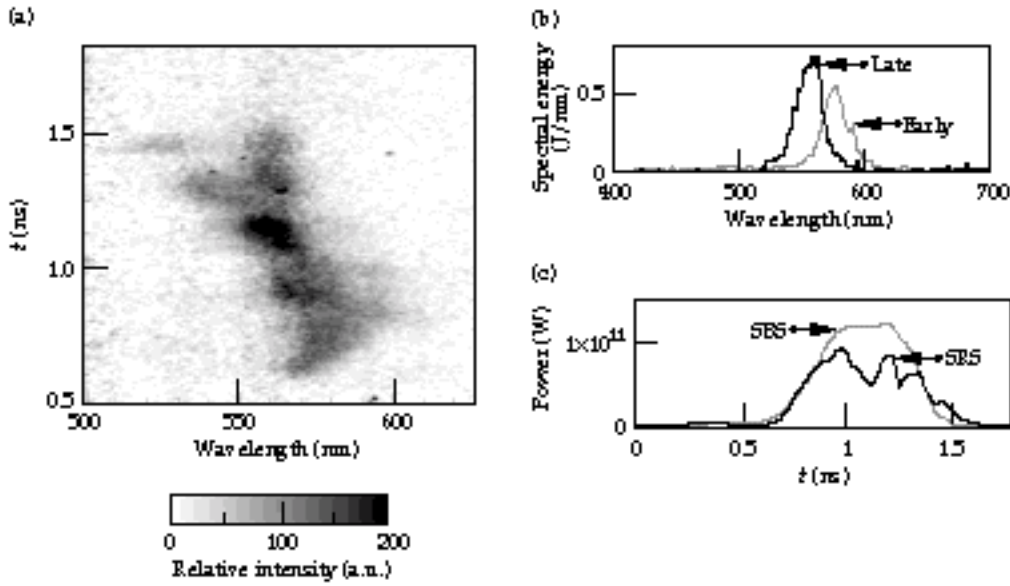
FIGURE 2. (a) A streaked spectrum of the SRS reflectivity from a target with 5.5% impurity concentration shows a narrow line consistent with a flat density profile before 1.0 ns and a decreasing density after 1.0 ns. (b) Time-integrated reflectivity from (a) shows a narrow peak at 575 nm in the 0.5- to 1.0-ns "early" period. (c) The spectrally integrated power collected by the SRS and SBS detectors is shown for the case in (a). (08-00-0797-1245pb01)

damping rate of the ion-acoustic wave. The integrated energies from the two time periods are expressed as percent reflectivities of the incident beam power due to SRS, and are plotted in Figure 3. A similar analysis has been done for backscattered light between 350.5 and 352 nm, w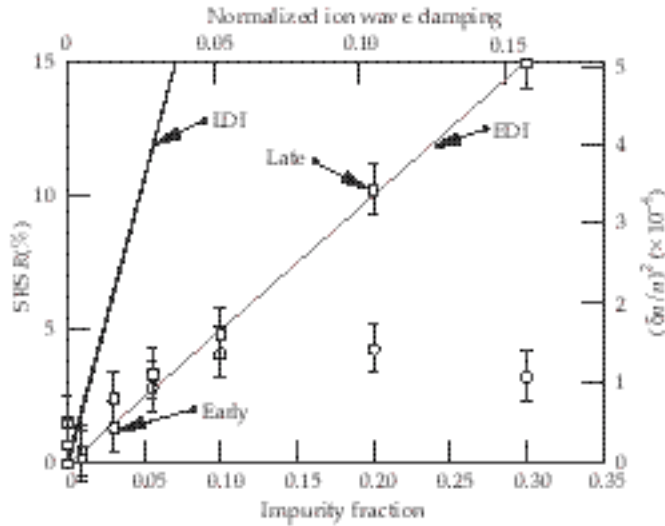hich is interpreted as SBS backscatter as described in Ref. 14. The integrated data clearly show that late-time SRS reflectivities are approximately proportional to the impurity concentration for all concentrations studied. The early-time reflectivities are proportional to concentration up to 10% and become independent, or a mildly decreasing function, of concentration between 10% and 30%. Because the ion-acoustic damping rate is expected to be linear with impurity concentration in this case,[23] a linear dependence of reflectivity on impurity concentration is interpreted as a linear dependence on the damping of the ion-acoustic wave. The possibility that dependence of the reflectivity on ion-wave damping is actually the result of suppression of SRS by large-amplitude ion waves generated by SBS (as discussed in Refs. 3 and 4 and references therein) is unlikely, because the observed dependence of SBS on ion-wave damping is weak in this case.[14]

These observations are the first demonstration of the direct dependence of SRS reflectivity on the damping rate of the ion-acoustic wave. In particular, the early-time reflectivity for concentrations between 1% and 10% demonstrates SRS increasing with ion-wave damping when the electron–ion collision rate, electron temperature, radiated power, and SBS level are essentially constant. In addition, the early-time reflectivity at higher concentration is nearly independent of the ion-wave damping rate, suggesting that the reflectivity falls below the threshold scaling law when the ion-wave damping is strong. Two types of plasma are expected in the NIF: a hot Au plasma near the hohlraum wall and a hot low-Z plasma in the hohlraum interior. These types of plasma correspond to the early-time plasma

FIGURE 3. SRS reflectivities averaged over the 0.5- to 1.0-ns "early" period and the 1.0- to 1.5-ns "late" period are shown vs impurity concentration. The impurity concentration is interpreted as the ion-wave damping rate (top axis), and the reflectivity is interpreted as the square of the fluctuation amplitude (right axis). Black and gray lines represent the LDI and EDI threshold amplitudes for a uniform beam and parameters relevant to early-time data. The LDI limited reflectivity in a nonuniform beamcan be much lower than what is shown (see text). (08-00-0797-1246pb01)

conditions at the two extremes of the ion-wave damping axis in Figure 3, which suggests that the SRS will be at correspondingly low levels in the NIF hohlraum.

Comparison with Models of Secondary Decays Involving Ion Waves

A simple model is presented to show how the observed dependence of the reflectivity on ion-wave damping may be explained by secondary decay of the Langmuir wave. In this model, the intensity profile of the beam and filamentation are neglected for simplicity, and the Langmuir wave amplitude is assumed to be in the vicinity of the threshold for the secondary decay. This threshold for decay, expressed in terms of the density fluctuation, is given by Ref. 9 for LDI and by Ref. 13 for EDI,

$$\left. \frac{\delta n_{e}}{n_{e}} \right|_{EDI} = 4 \, k_{L} \, \lambda_{De} \left(\frac{\nu_{ia}}{\omega_{ia}} \right)^{0.5} \left(\frac{\nu_{em}}{\omega_{p}} \right)^{0.5} , \qquad (1a)$$

$$\left. \frac{\delta n_{e}}{n_{e}} \right|_{LDI} = 4 \, k_{L} \, \lambda_{De} \left(\frac{\nu_{ia}}{\omega_{ia}} \right)^{0.5} \left(\frac{\nu_{L}}{\omega_{p}} \right)^{0.5} , \qquad (1b)$$

where k_{L} is the wave vector of the SRS-generated Langmuir wave, ν_{ia}/ω_{ia} is the normalized linear ion-wave damping rate, ν_{em} is the linear damping rate of the EDI, ν_{L} is the linear damping rate of the LDI, and λ_{De} is the electron Debye length. The measured SRS light is interpreted as Thomson scattering off density fluctuations in the scattering volume using the following assumptions. For these experiments the rapid collisional absorption rate of the incident and reflected light determines the size of the interaction region that can be viewed by the backscatter diagnostic. The effective length L used is the depth at which the attenuation of an incident 351-nm light times the attenuation of the reflected 580-nm light is equal to $1/e$. L is 300 μm, which in this case indicates that the observed SRS comes primarily from the plasma at radii larger than 1 mm. For perfectly coherent fluctuations, the reflectivity is proportional to this length to the second power,[10] but the finite spectral width observed in Figure 2 ($\delta k \approx 5.6 \times 10^{5} \, m^{-1}$) indicates that in this experiment the maximum distance over which the radiation can be coherent is given by $\ell_{c\,max.} = 1/\delta k$. A finite correlation length will reduce the reflectivity by a factor of at least $\ell_{c\,max}/L$ (Ref. 8) below the value for coherent

fluctuations, giving the maximum reflectivity R for a uniform beam as

$$R_{max} = \frac{1}{4} \left(\frac{n_{e}}{n_{c_{0}}} \right)^{2} k_{0}^{2} L (\delta k)^{-1} \left(\frac{\delta n_{e}}{n_{e}} \right)^{2} , \qquad (2)$$

where k_{0} and $n_{c_{0}}$ are the wave number and critical density of the incident beam. This model indicates that the SRS reflectivity is linearly proportional to ion-wave damping if the Langmuir wave amplitude does not grow significantly above the secondary decay threshold. This linear dependence is most clearly observed in the reflectivity data taken at early time when the impurity concentration is less than 10%. For impurity concentrations above 10%, the early-time reflectivity is not very dependent on the ion-wave damping. This is likely due to the convective saturation of the SRS-generated Langmuir wave before it reaches the secondary decay threshold. The secondary decay mechanism will only determine the SRS reflectivity when the primary three-wave process is sufficiently strong to drive the Langmuir wave amplitude to the threshold for the secondary decay. Thus at early time and high impurity concentration (>10%), the secondary decay threshold is sufficiently high that the SRS reflectivity is likely limited by the convective saturation of the three-wave SRS process and is therefore observed to be approximately independent of ion-wave damping. The late-time data show linear dependence of the reflectivity on the impurity concentration up to much higher concentration. This may be because at late time the plasma has cooled and therefore has a higher convective saturation level for the three-wave process, resulting in reflectivities that follow the linear scaling with ion-wave damping up to at least 30%, as shown in Figure 3. However, quantitative analysis of the late-time data is complicated by variations of the plasma properties in time and space.

As an additional check of the model of secondary decay, the density perturbation is estimated from the measured reflectivity at early time using Eq. (2), and is compared with that predicted by Eqs. (1a) and (1b). To evaluate Eqs. (1a) and (1b), the damping rates[24] of the Langmuir and electromagnetic waves are calculated using the distribution function expected in a high-Z plasma illuminated with high-intensity light.[25] The thresholds are evaluated assuming the average beam intensity ($3.0 \times 10^{15} \, W/cm^{2}$) exists throughout the interaction region and are shown as black and gray lines in Figure 3. In this case the equilibrium distribution is a super-Gaussian with $n = 3.5$ (where $n = 2$ corresponds to a Maxwellian). The estimate shown for the EDI threshold is not changed significantly by

inhomogeneities in the beam profile (i.e., hot spots), but the estimate for LDI may be significantly reduced by inhomogeneities. This reduction results from the fact that the Langmuir-wave Landau damping is strongly sensitive to intensity, as discussed in Ref. 24, so that in a hot spot the threshold density fluctuation will be much lower and the gain of the three-wave SRS process will be much higher. As a result, in a nonuniform beam, LDI may be significantly affecting the SRS even when the reflectivity is well below the uniform beam threshold. Comparison of these estimates with data indicates that the average fluctuation amplitudes observed in the experiment at early times and when the impurity concentration is between 0% and 10% are large enough to excite EDI over much of the beam profile and LDI in intense regions of the beam.

Conclusion

We have observed that the SRS reflectivity in a high-Z plasma is dependent on the ion-wave damping when the Langmuir wave properties are held constant, implying that SRS is limited by a process involving ion-acoustic waves. Furthermore, the observed reflectivities are linear with ion-wave damping as expected when the electron-wave amplitude is limited by EDI or LDI, and the observed wave amplitudes are near or above the thresholds for those instabilities, indicating that the SRS reflectivity in the NIF is likely to be limited by these secondary decay processes.

Acknowledgments

Notes and References

1. J. Lindl, *Phys. of Plasmas* **2**, 3933 (1995).
2. W. L. Kruer, *The Physics of Laser Plasma Interactions* (Addison–Wesley Publishing Co., Redwood City, CA, 1988).
3. C. J. Walsh, D. M. Villeneuve, and H. A. Baldis, *Phys. Rev. Lett.* **53**, 1445 (1984).
4. H. A. Baldis, et al., *Phys. Rev. Lett.* **62**, 2829 (1989).
5. H. A. Rose, D. F. DuBois, and B. Bezzerides, *Phys. Rev. Lett.* **58**, 2547 (1987).
6. K. Estabrook, W. L. Kruer, and M. G. Haines, *Phys. Fluids B* **1**, 1282 (1989).
7. T. Kolber, W. Rozmus, and V. T. Tikhonchuk, *Phys. Fluids B* **5**, 138 (1993).
8. T. Kolber, W. Rozmus, V. T. Tikhonchuk, *Phys. Plasmas* **2**, 256 (1995).
9. S. J. Karttunen, *Phys. Rev. A* **23**, 2006 (1981).
10. J. A. Heikkinen and S. J. Karttunen, *Phys. Fluids* **29**, 1291 (1986).
11. R. P. Drake and S. H. Batha, *Phys. Fluids B* **3**, 2936 (1991).
12. B. Bezzerides, D. F. DuBois, and H. A. Rose, *Phys. Rev. Lett.* **70**, 2569 (1993).
13. K. L. Baker, Ph.D. Dissertation, University of California, Davis (1996); see also P. K. Shukla et al., *Phys. Rev. A* **27**, 552 (1983).
14. R. K. Kirkwood et al., *Phys. Rev. Lett.* **77**, 2706 (1996).
15. R. K. Kirkwood et al., *Phys. of Plasmas* **4**, 1800 (1997).
16. J. C. Fernandez et al., *Phys. Rev. Lett.* **77**, 2702 (1996).
17. D. H. Kalantar et al., *Phys. of Plasmas* **2**, 3161 (1995).
18. C. A. Back, personal communication.
19. G. Zimmerman and W. Kruer, *Comments in Plasma Phys. and Controlled Fusion* **2**, 85 (1975).
20. J. D. Moody et. al., *Bull. Am. Phys. Soc.* **39**, 1753 (1994).
21. H. N. Kornblum, R. L. Kauffman, and J. A. Smith, *Rev. Sci. Inst.* **57**, 2179 (1986).
22. R. K. Kirkwood et al., *Rev. Sci. Inst.* **68**, 636 (1997).
23. E. A. Williams et al., *Phys. of Plasmas* **2**, 129 (1995).
24. B. B. Afeyan, W. L. Kruer, and A. E. Chou, "New Regimes of Parametric Instabilities in Plasmas with Super Gaussian Velocity Distribution Functions," Lawrence Livermore National Laboratory, Livermore, CA, UCRL-JC-125364; submitted to *Phys. Rev. Lett.*, and in this *Quarterly Report*, p. **XX**.
25. P. Alaterre, J.–P. Matte, and M. Lamoureaux, *Phys. Rev. A* **34**, 1578 (1986); A. B. Langdon, *Phys. Rev. Lett.* **44**, 575 (1980).